Article

Site-Selective Metal Binding by Designed □-Helical Peptides

Manolis Matzapetakis, and Vincent L. Pecoraro

J. Am. Chem. Soc., **2005**, 127 (51), 18229-18233• DOI: 10.1021/ja055433m • Publication Date (Web): 02 December 2005

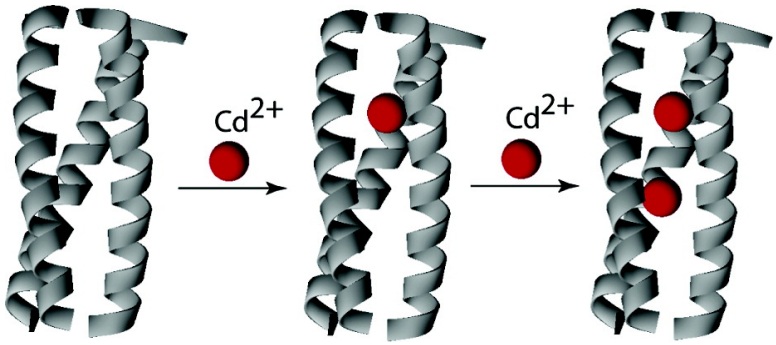

J|A|C|S
ARTICLES
Published on Web 12/02/2005

Site-Selective Metal Binding by Designed α-Helical Peptides

Manolis Matzapetakis† and Vincent L. Pecoraro*

Contribution from the Department of Chemistry and Department of Biophysics, University of Michigan, Ann Arbor, Michigan 48109-1055

Received August 9, 2005; E-mail: vlpec@umich.edu

Abstract: It is known that the designed α-helical peptide family TRI [(Ac-G(LKALEEK)$_4$G-CONH$_2$)], containing single site substitution of a cysteine for a leucine, is capable of binding Cd(II) within a three-stranded coiled coil. The binding affinity of cadmium is dependent upon the site of substitution, with cysteine incorporated at the **a** site leading to cadmium complexes of higher affinity than when a **d** site was modified. In this work we have examined whether this differential binding affinity can be expressed in a di-cysteine-substituted peptide in order to develop site specificity within a designed system. The peptide TRI L9CL19C was used to determine whether significant differences in binding affinities at nearly proximal sites could be achieved in a short designed peptide. On the basis of ^{113}Cd, ^{1}H NMR, and circular dichroic spectroscopies, we have shown that 1 equiv of Cd(II) binds exclusively at the **a** site. Only after that position is filled does the second site become populated. Thus, the TRI system represents the first example where stoichiometrically equivalent peptides with different sequences form the framework for designing molecular assemblies that show site-specific ion recognition. We propose that the distinct metal affinities are due to the cysteine conformers at different substitution points along the peptide. Furthermore, we have shown that site selectivity in biomolecules can be encoded into relatively short peptides with helical sequences and, therefore, do not necessarily require the extensive protein scaffolds found in natural systems.

The transition from structural biology's great achievements in the field of atomic resolution protein structures to the understanding of the connection between primary sequence and protein structure and function has been facilitated by the relatively recent and fairly rapid development of the field of de novo protein design.[1−5] Examples where first principles have been used as the sole guidance to design desired tertiary and quaternary folds are increasing in numbers and continue to provide insight into the basic principles that govern protein structure. Yet the more ambitious goal of designing functional proteins and peptides, with the goal of understanding the connection between structure and function, is only beginning to materialize.[6−11] One of the cornerstones of functional peptides is the ability to perform molecular recognition, something nature has mastered as shown with the extraordinary specificity various proteins exhibit for substrates and cofactors. The later case involves binding of metals as cofactors where very diverse coordination modes have been observed.[12] What has fascinated and puzzled researchers is how seemingly identical coordination environments can lead to altered catalytic activities,[13] altered metal structures,[14] or selective metal binding.[15] In these cases, the inherent design of the binding site is dictating the metal specificity.

To investigate the influence of the protein environment on metal specificity, we designed a system that would contain two sites with identical chemical composition but slightly different metal binding geometries and metal affinities. To achieve this goal we employed our knowledge of the design of heavy metal binding peptides using the TRI peptide series[16] G(LKALEEK)$_4$G, where a single leucine was converted into a cysteine. It was shown that when the cysteine substitution occurred in an **a** site (9, 16, or 23), a peptide with higher affinity for Hg(II) or Cd(II) was obtained than when the cysteine was placed into a **d** position (12 or 19).[17] We felt that we could exploit these

† Present address: Center for BioIron, Children's Hospital of Oakland Research Institute, Oakland, CA 94609.

(1) DeGrado, W. F.; Summa, C. M.; Pavone, V.; Nastri, F.; Lombardi, A. *Annu. Rev. Biochem.* **1999**, *68*, 779−819.
(2) Hill, R. B.; Raleigh, D. P.; Lombardi, A.; Degrado, N. F. *Acc. Chem. Res.* **2000**, *33* (11), 745−754.
(3) Bolon, D. N.; Voigt, C. A.; Mayo, S. L. *Curr. Opin. Chem. Biol.* **2002**, *6* (2), 125−129.
(4) Gibney, B. R.; Dutton, P. L. *Advances in Inorganic Chemistry*; Academic Press Inc.: San Diego, CA, 2001; Vol. 51, pp 409−455.
(5) Hodges, R. S. *Biochem. Cell Biol.* **1996**, *74* (2), 133−154.
(6) Baltzer, L.; Nilsson, J. *Curr. Opin. Biotechnol.* **2001**, *12* (4), 355−360.
(7) Doerr, A. J.; Case, M. A.; Pelczer, I.; McLendon, G. L. *J. Am. Chem. Soc.* **2004**, *126* (13), 4192−4198.
(8) Case, M. A.; McLendon, G. L. *Acc. Chem. Res.* **2004**, *37* (10), 754−762.
(9) Kaplan, J.; DeGrado, W. F. *Proc. Natl. Acad. Sci. U.S.A.* **2004**, *101* (32), 11566−11570.
(10) Kennedy, M. L.; Gibney, B. R. *Curr. Opin. Struct. Biol.* **2001**, *11* (4), 485−490.
(11) Nanda, V.; Rosenblatt, M. M.; Osyczka, A.; Kono, H.; Getahun, Z.; Dutton, P. L.; Saven, J. G.; Degrado, W. F. *J. Am. Chem. Soc.* **2005**, *127* (16), 5804−5.
(12) Reedy, C. J.; Kennedy, M. L.; Gibney, B. R. *Chem. Commun.* **2003** (5), 570−571.
(13) Miller, A. F. *Cerr. Opin. Chem. Biol.* **2004**, *8* (2), 162−168.
(14) Du Bois, J.; Mizoguchi, T. J.; Lippard, S. J. *Coord. Chem. Rev.* **2000**, *200*, 443−485.
(15) Hart, P. J.; Balbirnie, M. M.; Ogihara, N. L.; Nersissian, A. M.; Weiss, M. S.; Valentine, J. S.; Eisenberg, D. *Biochemistry* **1999**, *38* (7), 2167−2178.
(16) Dieckmann, G.; McRorie, D.; Tierney, D.; Utschig, L.; Singer, C.; OHalloran, T.; Penner-Hahn, J.; DeGrado, W.; Pecoraro, V. *J. Am. Chem. Soc.* **1997**, *119* (26), 6195−6196.
(17) Matzapetakis, M.; Farrer, B. T.; Weng, T.-C.; Hemmingsen, L.; Penner-Hahn, J. E.; Pecoraro, V. L. *J. Am. Chem. Soc.* **2002**, *124* (27), 8042−8054.

differential metal affinities found in monocysteine-containing cysteines to realize a short peptide with two metal binding sites that could bind metals with different strengths. In this paper we present the result of these studies that demonstrate that it is possible to achieve such selectivity in a relatively simple system.

Materials and Methods

Fmoc-protected amino acids and the MBHA rink amide resin were purchased from Novabiochem; *N*-hydroxybenzotriazole (HOBT) and 2-(1*H*-benzotriazol-1-yl)-1,1,3,3-tetramethyluronium hexafluorophosphate (HBTU) were bought from Anaspec Inc.; diisopropylethylamine (DIEA), acetic anhydride, and pyridine were purchased from Aldrich; and piperidine was supplied by Sigma. *N*-Methylmorphopyridinone (NMP) was from Fisher Scientific.

Peptide Synthesis and Purification. Peptides were synthesized on an Applied Biosystems 433A automated peptide synthesizer, with Fmoc-protected amino acids by use of the FastMoc activation protocol (Applied Biosystems). Rink amide MBHA resin was used as the solid support so that the resulting peptides would be amidated at the C-terminus. The N-terminus was acetylated on the column with a solution of 4% (v/v) acetic anhydride, 4.3% pyridine, and 91.7% *N*,*N*-dimethylformamide (DMF). Cleavage from the resin was performed for 90 min in a 90% trifluoroethanol (TFA) solution containing 5% anisole, 3% thioanisole, and 2% ethanedithiol as free radical scavengers. After precipitation with cold ether, the peptide was redissolved in water and lyophilized to obtain a fluffy off-white powder. The solid was redissolved in 10% acetic acid and purified by reversed-phase HPLC on a Waters 600 Semiprep HPLC with a preparative C18 column (Vydac protein & peptide) with a linear gradient of 0.1% TFA in water to 0.1% TFA in 9:1 CH_3CN/H_2O over 50 min. The identity of the peptides was verified by MALDI-TOF (matrix-assisted laser desorption ionization time-of-flight) and ES (electrospray) mass spectrometries (expected MW = 3411, found 3411.52), and the purity was determined by analytical HPLC to be greater than 90%. The peptide concentration of these solutions was determined by quantitation of the cysteine thiols by Ellman's test,[18] which uses the product of the reaction of the aliphatic thiols with dithionitrobenzoate (DTNB) as a spectroscopic probe.

CD Spectroscopy. CD spectroscopy was performed on an Aviv 202 CD spectrophotometer with the temperature regulated at 298 K. Spectra were collected from 300 to 230 nm every 1 nm with 1 s for signal averaging. The molar ellipticity, [Θ], is given in units of degrees centimeter^2 decimole^{-1}.

Guanidine hydrochloride (GuHCl) titrations were carried out on the same instrument, equipped with a Hamilton automatic titrator, monitored at 222 nm with data collected after 1 s averaging and 2.5 min waiting time under stirring between each data point collection. During the titration, appropriate volumes of the initial solution of 5 mM phosphate at pH 2.5 or 8.5 and 10 μM peptide were automatically mixed with an 8.6 M GuHCl solution containing the same amount of peptide and buffer to obtain each desired condition.

UV Spectroscopy. UV absorption data were recorded on a Perkin-Elmer Lambda 9 UV−vis−NIR spectrophotometer in the range of 300−220 nm. Aliquots of a 10 mM $CdCl_2$ stock solution were titrated in a cell containing 30 mM peptide solution in Tris-H_2SO_4 buffer at pH 8.5.

NMR Spectroscopy. ^{113}Cd spectra were collected on Bruker AMX 500 and Varian Inova 500 spectrometers, equipped with broadband probes. All spectra were collected at room temperature and were externally referenced to 0.1 M $Cd(ClO_4)_2$ solution in D_2O. A spectral width of 800 ppm (93 876 Hz) was sampled with 64 000 or 120 000 points. The number of scans varied per spectrum, ranging from 1000 to 4000. A 0.5 s delay was introduced between scans, which, coupled with the 1 s acquisition time, resulted in a 1.5 s total delay for the relaxation of the nuclei. A 60° pulse (5.5 μs) was used. For these experiments, samples were prepared by dissolving 35 mg of peptide in 0.500 mL of degassed (bubbled with Ar) D_2O, followed by the desired amount of 500 mM $^{113}CdCl_2$ solution (Cambridge Isotopes) and adjustment of the pH with KOH or HCl solutions. No buffer was used, and the pH was checked before and after the measurements and was not found to change. An argon atmosphere was maintained when possible, but the samples came in contact with O_2 while the pH was adjusted. The resulting samples contained 15 mM peptide that corresponds to 5 mM three-helix coiled coil. The 1D data were processed with the software Mestrec v2.3a. All free induction decays (FIDs) were zero-filled to double the original points and were treated with an exponential function with a line broadening of 50 Hz. After phasing, the data were baseline-corrected by use of a 6th-degree polynomial function.

All the 2D experiments were performed on a Bruker AMX500 spectrometer equipped with a broadband reverse probe. Samples were prepared by dissolving about 20 mg of lyophilized and degassed peptide in 500 μL of 10% D_2O under a flow of argon. Cadmium was added in the form of $^{113}CdCl_2$ where needed, and the pH was adjusted with solutions of KOH and HCl by use of a Hamilton NMR pH electrode connected to an Fisher Accumet 805MP pH meter. Nuclear Overhauser effect spectroscopy (NOESY) was performed with the standard Bruker pulse sequences, with presaturation for 1.5 s (55 dB power) for water suppression in the States acquisition mode. A mixing time of 100 ms was used in all cases. For the unmetalated samples, a 12 ppm window was sampled with 2048 points and 1024 increments in the indirect dimension with 24 scans. Total correlation spectroscopy (TOCSY) data were collected under similar conditions with a 7 kHz 90° pulse (14 dB) for the Waltz16 pulse sequence. A 60 ms spin lock was used throughout. For the rest of the metalated samples, lower resolution NOESY spectra were collected with only 512 or 256 increments and eight scans. The data were processed with the program nmrPipe, and peak picking was performed with SPARKY.

Table 1. Primary Sequences of Peptides of the TRI Family

	1 5 10 15 20 25 30
TRI	$CH_3(C=O)$-GLKALEEKLKALEEKLKALEEKLKALEEKG-NH_2
TRI L9C	$CH_3(C=O)$-GLKALEEK**C**KALEEKLKALEEKLKALEEKG-NH_2
TRI L19C	$CH_3(C=O)$-GLKALEEKLKALEEKLKA**C**EEKLKALEEKG-NH_2
TRI L9CL19C	$CH_3(C=O)$-GLKALEEK**C**KALEEKLKA**C**EEKLKALEEKG-NH_2

Results and Discussion

Our approach was to use the host peptide, referred to as TRI (see Table 1), that is based on a repeated heptad design[16] and forms trimeric α-helical coiled coils above pH 5 in solution. These trimers are ideal scaffolds for a metal binding site arising from the placement of a metal binding residue in the center of these systems. The core is composed of leucine residues at positions **a** and **d** of each heptad. Replacement of a single leucine for a cysteine at either **a** or **d** position has yielded peptides with binding sites for heavy metals such as Cd(II) and Hg(II). These metals are bound in unfavorable yet biologically significant trigonal planar coordination geometries.[16] However, the placement of the cysteines in different positions of the core yielded similar yet distinctly different metal sites.[17,19] We found that metals uniformly bound preferentially to **a** rather than **d** sites. While we were able to measure a binding constant of cadmium for the **d** site (3×10^9 M^{-1}), the binding affinity of cadmium for the **a** site was too great for quantitative determi-

(18) Ellman, G. L. *Arch. Biochem. Biophys.* **1958**, *74* (2), 443−450.

(19) Dieckmann, G.; McRorie, D.; Lear, J.; Sharp, K.; DeGrado, W.; Pecoraro, V. *J. Mol. Biol.* **1998**, *280* (5), 897−912.

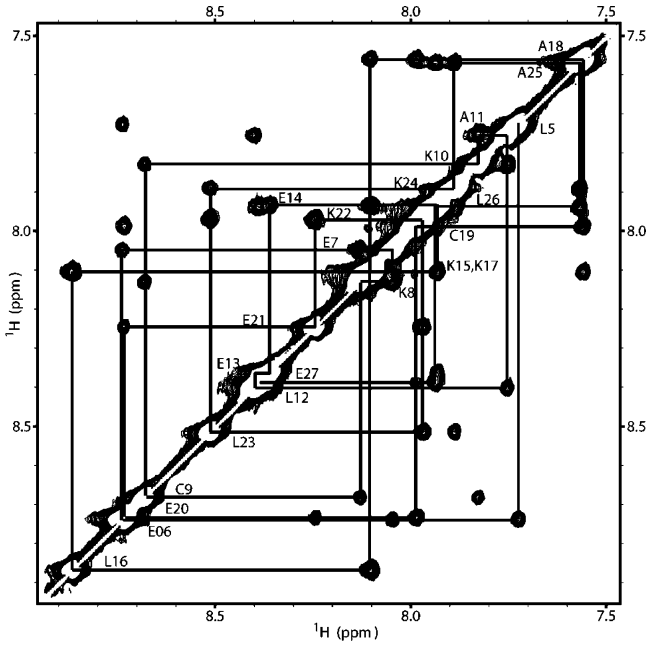

Figure 1. Amide region section of the NOESY spectrum of a 3 mM (TRI L9CL19C)$_3$ solution in 10% D_2O at pH 8.5, showing the sequential assignment of the amide protons. The NOEs are characteristic for α-helical peptides.

nation, placing the **a** site binding constant at least an order of magnitude greater than that for the **d** position.[17] Furthermore, we found that the metal in those systems was in equilibrium between a trigonal and a tetrahedral geometry with slightly different trigonal:tetrahedral ratios in **a** versus **d** positions. We showed that the ^{113}Cd NMR chemical shift provides a very good indication of the ratio of the two geometries present in the system.[20,21] Table 1 illustrates that TRI L9C and TRI L19C have identical chemical composition, differing only at the location of the cysteine substitution. The observation that such conservative peptide modifications could lead to significant changes in metal discrimination led us to believe that we could take advantage of this subtle sequence difference to create the first model peptide containing apparently identical metal binding sites with distinctly different metal affinities.

We decided to place the cysteines at positions 9 (**a**) and 19 (**d**) so that they are in the center of the peptide, while they are separated by the leucine layer of position 16 to avoid interactions between the sites. The resulting peptide, TRI L9CL19C, was synthesized by solid-phase peptide synthesis as described previously[17] and was found to be helical and stable in solution as shown from CD-monitored guanidine hydrochloride titrations. Furthermore, it exhibited a very well-defined structure, contrary to cases of molten globules, as we can deduce from the dispersion of the proton NMR and our ability to assign the backbone resonances of at least 26 of the 30 amino acids in the 2D NOESY spectrum (see Figure 1). Because these peptides exist as trimers in solution (under the conditions we are investigating),[19] they will be described as (TRI L9CL19C)$_3$ in solution studies.

Having established the solution behavior of the unmetalated system, we looked at its metal binding properties. Difference

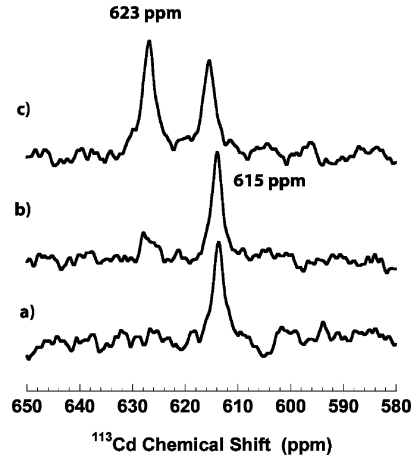

Figure 2. ^{113}Cd NMR spectra of 4 mM (TRI L9CL19C)$_3$ at pH 8.5 with (a) 0.9, (b) 1.1, and (c) 2 equiv of $^{113}CdCl_2$.

UV titrations, monitoring the ligand to metal charge transfer (LMCT) bands associated with the formation of the metal−sulfur bond at 231 nm, indicated that two metals were binding to each peptide trimer. Thus, the first objective of designing multiple binding sites was a success. We further characterized the metal binding of TRI L9CL19C using ^{113}Cd NMR, an excellent probe for the Cd environment. The ^{113}Cd chemical shift is very sensitive to coordination number and ligand type, with oxygen ligands exhibiting a dramatically different chemical shift compared to sulfur.[20] Additionally, direct detection of each site can be possible if the two sites are both sufficiently different and if the metal does not migrate between the sites faster than the NMR time scale. Titration of 1 equiv of $^{113}CdCl_2$ into a 9 mM peptide solution (3 mM of the trimer) at pH 8.5 showed a single peak appearing first at 615 ppm, followed by a second resonance on addition of the second Cd(II) equivalent, at 624 ppm (Figure 2). These signals were very informative. First, the chemical shifts are indicative of a primarily sulfur coordination environment for Cd(II) in either case.[20] Second, the appearance of two signals indicated two distinct noninterchanging environments for the metals. Finally, we saw that metal binding was quantitatively more favorable for one of the sites, with metal binding appearing to be at least 90% preferentially bound to one of the sites. However, the low sensitivity of ^{113}Cd NMR spectroscopy coupled with a small degree of peptide oxidation over the time of the experiment did not allow us to more fully quantify the differential binding. In addition, we were unable to establish the preferred binding site from this experiment.

To assign the metal site preference, we turned to circular dichroism (CD) spectroscopy. This method is able to detect electronic transitions that arise from chromophores found in chiral environments. It is often used for the identification of the secondary structure of proteins; however, it has also been used to study metal binding. We have shown that it is possible to observe LMCT bands in our system using CD even though the first coordination sphere of the metal is not chiral. We speculate that the extended chiral environment around the metal is inducing this effect. Furthermore, we have shown that metal binding to sites composed of cysteines in an all **a** or all **d** site configuration gives rise to spectra with opposite signs.[18] If this behavior holds true for the case of the disubstituted peptides, we have a direct method for distinguishing metal complexation to **a** versus **d** sites. As shown in the left panel of Figure 3, it is

(20) Hemmingsen, L.; Olsen, L.; Antony, J.; Sauer, S. P. A. *J. Biol. Inorg. Chem.* **2004**, *9* (5), 591−599.
(21) Lee, K. H.; Matzapetakis, M.; Mitra, S.; Neil, E.; Marsh, G.; Pecoraro, V. L. *J. Am. Chem. Soc.* **2004**, *126* (30), 9178−9179.

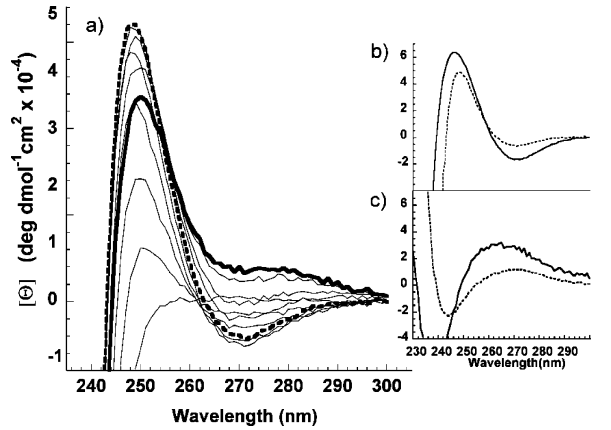

Figure 3. (a) CD titration of 10 μM (TRI L9CL19C)$_3$ in 10 mM Tris-H_2SO_4, pH 8.5, titrated with Cd(II): (---) 1 equiv;(—) 2 equiv. (b) Comparison of the signal with 1 equiv of metal (—) with that of a typical **a** site (---). (c) Comparison of the final spectrum (corrected for the absorbance of the first equivalent) (—) with that of a typical **d** site with Cd (---) (from ref 18).

clear that two different species are present during the titration with the first one (bold dashed line) growing to a maximum on addition of the first equivalent of metal at 249 nm and a minimum at 272 nm. Addition of the second equivalent of metal results in a new signal with decreased intensity at 249 nm and a consequent increase in intensity at 270 nm. Deconvolution of the two signals and comparison with those of typical **a** (right top panel) and **d** sites (right bottom panel) revealed the similarity of the first with that of an **a** site while the second was qualitatively similar to that of a **d** site. Therefore, from this experiment we concluded that the order of metalation was the **a** site (9) being filled first, followed by the metalation of the **d** site (19). We did not assess the helicity of the peptide in the presence of metals using the CD data at 222 nm since in this spectral region we have a significant contribution from the LMCT transition of the complexes.

Because CD is not a commonly used method for identifying metal binding site specificity, we used two-dimensional NMR to validate our previous results. Two-dimensional NOESY and TOCSY spectra were employed to assign the backbone of the peptide, and this information was used to identify the resonances of the β-methylene protons of each cysteine. NOESY spectra were used to monitor the progress of a titration of metal into the peptide by observing the effects on the cysteine side-chain resonances. Sections of the spectrum containing the cross-peaks between the cysteine amide proton and their corresponding β-methylene protons are shown in Figure 4. On the horizontal axis we have the region corresponding to the amide protons, while on the vertical axis we observe the β-methylene protons of the two cysteines. The two peaks corresponding to each amide proton are due to the two nonequivalent β-methylene protons. The two additional sets of peaks at 7.85 and 8.75 ppm correspond to the interresidue cross-peaks between the amides of K10 and H^β of C9 and between H^N of E20 and H^β of C19, respectively. These peaks contain redundant information with areas a and c of the figure (therefore, they have been made lighter in color for simplicity).

Sequential additions of ^{113}Cd aliquots caused significant changes in the spectrum. The first additions of 0.5 equiv of metal resulted in the appearance of two new sets of amide resonances, one at 7.93 ppm, marked as d in Figure 4, and one at 8.29 ppm, marked as b. The latter ones were split in a manner characteristic of a $^3J(^{113}Cd-{}^1H^\beta)$ coupling.[22] The coupling constants of 16 and 43 Hz for each methylene proton are consistent with $^{113}Cd-{}^1H^\beta$ coupling (0−55 Hz) and are indicative of metal binding.[22] In contrast, the cross-peaks at 7.93 ppm exhibited no splitting or line broadening, while the β-methylene proton resonances were the same as those at 7.99 ppm, leading us to believe that they do not correspond to a new metal-bound species but rather to the unmetalated C19 site of the peptide that is slightly perturbed by metalation at the 9 position.

The next aliquot brought the metal concentration to 1.3 equiv of metal per (TRI L9CL19C)$_3$. The changes that were observed included the disappearance of the peaks at lines a and c, indicating that all of the unmetalated (TRI L9CL19C)$_3$ had been consumed at this point. At the same time, the peaks at b and d were fully developed while a new species started to appear at e at 7.83 ppm with methylene resonances at 3.15 ppm. That signal was assigned to the dimetalated peptide. Last, when the concentration of metal reached 2 equiv, relative to the peptide trimer, we observed that the peak at d had completely disappeared while the species at e had fully developed. The final β-methylene resonances centered at 3.18 ppm were also split by a $^3J(^{113}Cd-{}^1H^\beta)$ of 31 Hz while, a new peak at 2.91 ppm appeared. The second peak did not exhibit a measurable $^3J(^{113}Cd-{}^1H^\beta)$ splitting.

$^3J(^{113}Cd-{}^1H^\beta)$ couplings have been used in the past to extract $C^\alpha-C^\beta-S^\gamma-Cd$ dihedral angles with mixed success. Inconsistent behavior has been observed in more than one case, and this discrepancy has been attributed to the complex electronic structure of Cd. It is also suggested that the available relationships hold true only for systems of the same type. Since there are no reported values for mononuclear $Cd-S_3$ species, we were skeptical about applying it.[24] However, it is safe to say that since the coupling values we measured are so different for each site, the way of binding of cadmium to the **a** or the **d** site is significantly different as well.

A summary of the above observations is given in Figure 5, where the normalized relative intensities of the peaks of the unmetalated sites are plotted as a function of the metal added. For a detailed description of the method used to obtain the normalized intensities used in this figure, see the Supporting Information section. In addition, the dashed lines are the theoretical model for selective binding of metal to site 9 followed by site 19. The available data agree very well with this model.

These results are consistent with the ^{113}Cd NMR titration described above, which showed a single signal for the first equivalent of the metal added, followed by development of a second signal when greater than 1 equiv of metal was present. The conclusion that the **a** site is occupied first, and exclusively, with cadmium is further supported by the circular dichroism titration (Figure 3), where the spectrum typical of the **a** site substitution pattern is displayed throughout the addition of the first equivalent of metal. These experiments, which probe different physical properties in and around the metal binding site, demonstrate the preference of the metal for the **a** site. To

(22) Zerbe, O.; Pountney, D. L.; Vonphilipsborn, W.; Vasak, M. *J. Am. Chem. Soc.* **1994**, *116* (17), 7957−7957.
(23) Kiyokawa, T.; Kanaori, K.; Tajima, K.; Koike, M.; Mizuno, T.; Oku, J. I.; Tanaka, T. *J. Pept. Res.* **2004**, *63* (4), 347−353.
(24) Baleja, J. D.; Thanabal, V.; Wagner, G. *J. Biomol. NMR* **1997**, *10* (4), 397−401.

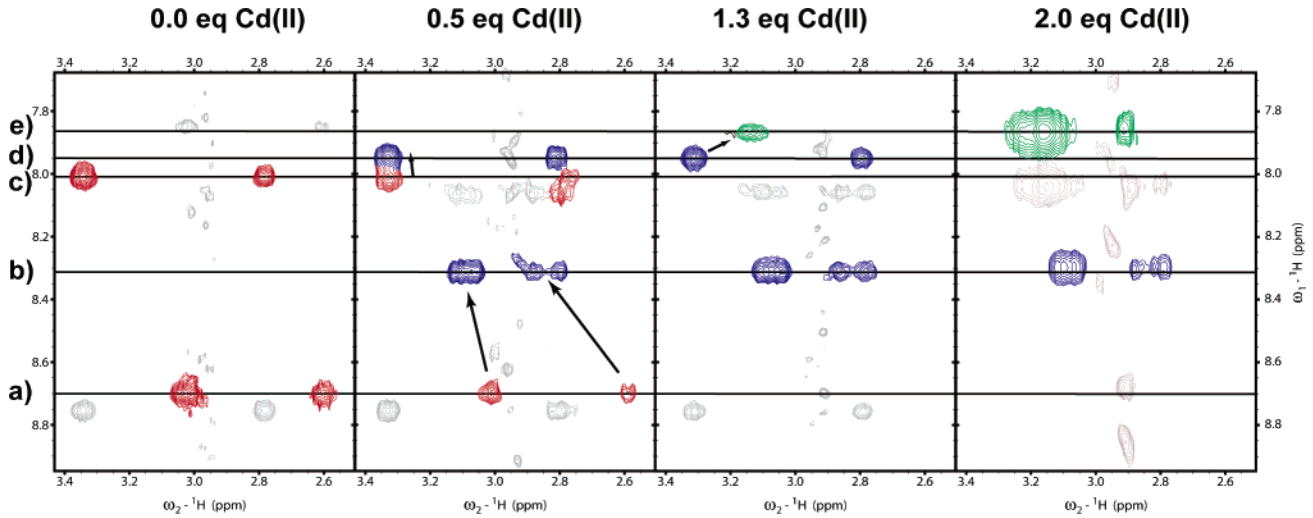

Figure 4. Sections of the ^{1}H−^{1}H NOESY spectra of TRI L9CL19C as a function of added equivalents of Cd(II). Colored peaks correspond to intraresidue NOEs of the amide protons (H^N) (horizontal axis) and the β-methylene protons ($H^{\beta 2/3}$) (vertical axis) of the cysteines. Other peaks, displayed in gray, are interresidue NOEs, (H^N_i−$H^{\beta 2/3}{}_{i+1}$) and we will not be referring to them. (a) $H^N{}_9$−$H^\beta{}_9$ for TRI(L9C)(L19C). (b) $H^N{}_9$−$H^\beta{}_9$ for TRI(Cd-L9C)(L19C) and TRI(Cd-L9C)(Cd-L19C). (c) $H^N{}_{19}$−$H^\beta{}_{19}$ for TRI(L9C)(L19C). (d) $H^N{}_{19}$−$H^\beta{}_{19}$ TRI(Cd-L9C)(L19C). (e) $H^N{}_{19}$−$H^\beta{}_{19}$ for TRI(Cd-L9C)(Cd-L19C).

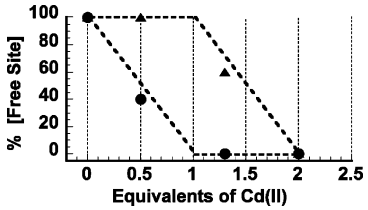

Figure 5. Plot of the relative concentrations of free C9 (●) and C19 (▲). The dotted lines represent the case of selective binding to site 9 followed by site 19.

observe such behavior, it is likely that the affinity of cadmium for the **a** site is at least an order of magnitude higher than that for the **d** site.

There are two structural possibilities that can lead to this site differentiation. The first possibility is that either a trigonal or tetrahedral cadmium ion binds more tightly than the other coordination geometry and that one site has a preference for the preferred geometry. The second alternative is that there is a metal ion preference based on the conformation of the amino acid ligand. We have previously shown that ^{113}Cd NMR spectroscopy can be used to estimate the ratio of 3- versus 4-coordinate cadmium at each site.[21] Since the chemical shift of ^{113}Cd, in our case, is the result of fast exchange between a Cd−S_3 and a Cd−S_3O species,[18] its value can be used to deduce the ratio of Cd−S_3 to Cd−S_3O. However, since the chemical shifts for the two sites do not differ significantly, we estimate that the **a** site ratio is 45:55 trigonal:tetrahedral, whereas that of the **d** site is 55:45. Clearly these ratios are not sufficiently different to explain an order of magnitude difference in the cadmium site affinity. Instead, we believe that the reason for this dramatically different behavior stems from the different conformers of each cysteine found in each type of site. The preferred rotamer for the side chain of a cysteine places the sulfur atom lone pair toward the center of the core (**a** type substitution) while the lone pair orientation is not as favorable in the case of a **d** substitution. A significant distortion is required in order to create a suitable metal binding environment. Thus, we believe that the energy penalty for the side-chain orientation in the case of the **d** site is translated in the reduced observed binding affinity.

Conclusion

To understand and unravel the principles that govern metalloprotein structure and function, we designed a system, using simple principles, that would simulate the naturally occurring metal specificity observed in many biological systems. While examples of such behavior exist in the literature,[23] they are due to the different ligand environments that these systems employ. A more challenging objective is to obtain significant metal ion specificity by use of the same first coordination sphere ligands and solely varying the conformation and environment of the metal binding cavity. Such studies allow us to evaluate the importance of the placement of metal binding residues in the primary sequence of the peptide and investigate their effects on the secondary and quaternary structure of the system.

By exploiting our previous observation that we could influence the metal binding affinity in trimeric coiled coil peptides by placing cysteine in different sites of the repeated heptad, we have now demonstrated that we can construct peptides with multiple metal binding regions that are capable of sequentially and selectively binding cadmium to those sites. Cysteines placed in the type **a** sites bound metal first, followed by metal binding in the **d** type sites. This behavior is likely due to energetic penalties associated with metal complexation when the cysteine sulfur lone pairs are not properly oriented in one conformation to form an optimal trigonal environment for the metal. Thus, we have shown that site selectivity in biomolecules can be encoded into relatively short peptides with helical sequences and, therefore, do not necessarily require the extensive protein scaffolds found in natural systems.

Acknowledgment. We thank Debdip Ghosh and Dr. Kyung-Hoon Lee for useful discussions and the National Institute of Health (Grant 5 R01 ES012236) for support of this work.

Supporting Information Available: Evaluation of the relative intensities from NOESY titration and figure showing guanidine hydrochloride denaturation titration of TRI L9CL19C. This material is available free of charge via the Internet at http://pubs.acs.org.

JA055433M